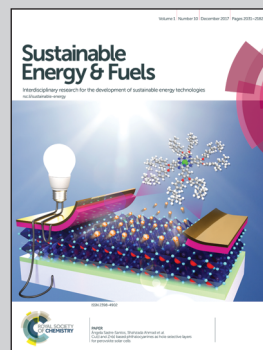


Showcasing research from Imperial College London

Solvent selection and design for CO₂ capture - how we might have been missing the point

In any sorbent-based separation process, decisions made at the molecular scale dictate the design and economics of the process in which it is used. There is a significant effort to develop improved sorbents for CO₂ capture. This research bridges the molecular and process scales and expresses the implications of molecular-level decisions on process economics. In this study, we focus on chemisorption using aqueous mixtures of organic solvents and identify the impact of thermophysical and kinetic solvent properties on process cost.

As featured in:



See Niall Mac Dowell *et al.*,
Sustainable Energy Fuels,
2017, 1, 2078.



rsc.li/sustainable-energy

Registered charity number: 207890



Cite this: *Sustainable Energy Fuels*,
2017, 1, 2078

Solvent selection and design for CO₂ capture – how we might have been missing the point

Maria T. Mota-Martinez, ^{abc} Jason P. Hallett ^a and Niall Mac Dowell ^{*bc}

Carbon capture and storage (CCS) is a vital technology for the cost-effective mitigation of anthropogenic CO₂ emissions. However, a key obstacle to its deployment on a large scale remains its cost – both capital and operating costs. In this context, the development of improved sorbents is a key research priority. Consequently, there is a vast global effort to develop new materials for this purpose, with literally thousands of new materials having been proposed since the beginning of the millennium. One common element of these contributions is that they focus on the equilibrium capacity of the material to absorb CO₂ and rarely, if ever, other key factors such as transport properties. To date, the majority of this effort has cost significant amounts of time and resources and has almost exclusively focused on developing sorbents with increased CO₂ capacity and/or reduced heat of regeneration. Given that sorbent regeneration largely dictates operational cost, this would, on the surface, appear rational. However, it is vital to recall that the cost structure of \$ per MWh of electricity generated is composed of contributions from both capital and operational costs. Consequently, this single-minded focus on equilibrium CO₂ capacity and heat of regeneration excludes the contribution of transport and kinetic properties which determine the equipment size and thus the capital cost. Therefore, in order to develop sorbents which will result in a non-negligible cost reduction, it is essential to move beyond equilibrium-based metrics of sorbent performance. In this paper, we present a new methodological approach for sorbent screening which explicitly includes rate-based phenomena. Our approach uses both monetised and non-monetised performance indicators. Our results suggest that whilst equilibrium CO₂ capacity is a key determinant of process performance, transport properties (e.g., viscosity) and other thermophysical properties (e.g., heat capacity) have a significant effect on the capital cost, and thus on the price of the carbon captured. The key contribution of this work is the identification of the minimum set of thermophysical and kinetic parameters which must be reported in order to justify the claim of adequacy for a new sorbent for CO₂ capture in particular and gas separations in general.

Received 16th August 2017
Accepted 21st August 2017

DOI: 10.1039/c7se00404d

rsc.li/sustainable-energy

1 Introduction

In 2014, the Intergovernmental Panel on Climate Change (IPCC) found that the cost of limiting the concentration of CO₂ equivalents in the atmosphere to 430–480 ppm would be 138% higher without a large scale deployment of carbon capture and storage (CCS) in the 2-degree scenario (2DS).¹ CCS technology is therefore key for the decarbonisation of the global economy. At the time of writing, 17 large demonstration plants are in operation, 5 projects are in the execution phase and another 5 are projected to be commissioned by 2020.^{2,3} Most of the CCS projects in operation encompass a wide range of CO₂ sources, including natural gas processing (9 projects), hydrogen

production (2 projects) and power generation (6 projects). Nonetheless, these plants will only capture a fraction of the total CO₂ that is required to meet the 2DS targets.[†] The current focus on the so-called 1.5 °C target associated with the 2015 Paris COP only serves to increase this ambition.[‡]

However, a common theme of all scenarios is that the commercial scale deployment of CCS is significantly behind schedule, relative to what was anticipated in the first decade of this millennium. It is commonly held that the capital and operating costs associated with CCS is a key impediment to its deployment. Accounting for approximately 60–70% of the cost per tonne of CO₂ avoided,⁴ the capture step is the most costly and energy intensive step of the CCS chain.⁵ Consequently, there is an intense focus on reducing the cost of the capture

^aDepartment of Chemical Engineering, Imperial College London, Exhibition Road, London, SW7 2AZ, UK

^bCentre for Process Systems Engineering, Imperial College London, Exhibition Road, London, SW7 2AZ, UK. E-mail: niall@imperial.ac.uk; Tel: +44 (0)20 7594 9298

^cCentre for Environmental Policy, Imperial College London, Exhibition Road, London, SW7 1NA, UK

[†] The CO₂ capture plants for power generation in operation at the time of writing in 2017 are Boundary Dam in Canada and Petra Nova in United States. The capture method in both cases is chemical absorption using amine.³

[‡] 40 Mtpa will be captured with the new capacity installed in 2017. The capacity required by 2040 is 4000 Mtpa².



process. Whilst the factors affecting the actual cost of a commercial-scale CCS project are many and varied,^{6,7} one key area where the research community can contribute is in the development of new materials and processes for the CO₂ capture. Chemical and physical absorption, adsorption,^{8–11} cryogenic separation,^{12,13} chemical and calcium looping^{14–17} and membranes¹⁸ are the technologies which are under active investigation for carbon capture. Nonetheless, chemical absorption using aqueous solutions of alkanolamines is the most mature technology for CO₂ capture, and the only one to have been deployed commercially in power plants thus far.^{3,19–21}

The cost per tonne of CO₂ captured (\$ per t_{CO₂}) is an aggregate of the equipment and plant construction, financing, fuel and other utility costs. The size and operating cost of the process equipment are functions of the thermophysical and chemical properties of the solvent. However, within the research community, there is an overwhelming focus on equilibrium properties which dictate the operating cost, to the exclusion of the properties which determine the size and thus the capital cost of process equipment. A substantial volume of work is dedicated to increasing the gas carrying capacity (*i.e.*, the CO₂ loading) or decreasing the enthalpy of absorption/desorption of the sorbent. This approach neglects the combined effects that the larger set of physicochemical, thermodynamic and transport properties of solvents have on the performance of the capture process, and therefore, on the cost. For example, the focus on reducing the enthalpy of absorption neglects the contribution of other properties such as the heat capacity and the enthalpy of vaporisation of the solvent to the thermal requirements in the regeneration step.²² For example, Oexmann and Kather argue that processes using solvents with higher heat of absorption can benefit from a higher pressure in the reboiler, resulting in lower power requirement in the compression stage prior to the CO₂ transport.²² Even in the event that a solvent reduces the energy per ton of CO₂ captured (GJ per t_{CO₂}) of the capture process, it does not mean that it reduces the overall cost of capture (\$ per t_{CO₂}), or more importantly, the cost of producing the low carbon product (\$ per MWh). A solvent with a low energy of regeneration could have inferior mass transfer characteristics, and thus could actually increase the \$ per MWh cost, despite having an improved GJ per t_{CO₂} figure. The size of the process units is directly linked not only to the thermodynamic but also to the transport properties of the solvent such as viscosity, thermal conductivity and diffusivity. The key question, therefore, is how these sorbent properties conspire to define a feasible parameter space which corresponds to a meaningful reduction in the total cost of carbon capture.

The answer to this question can only be obtained by a monetised process performance assessment. With this in mind, it is vital to identify the minimum set of properties which affect the cost of the carbon capture. Defining and optimising the operational envelop of these properties provide a space for evaluating the opportunities to design new solvents. It is equally important to have a reliable method for discriminating among candidate molecules using monetised and non-monetised key performance indicators (KPIs). Whilst the use of non-economic KPIs is useful for a preliminary sorbent screening effort, economic KPIs will likely determine the final viability of a candidate molecule.

In this paper we present a new methodology to assess the process performance of sorbents for carbon capture. We have developed a software tool that evaluates a range of selected KPIs based on the description of the reaction kinetics, thermodynamics, and transport properties of the solvent. Our tool includes a description of the chemical equilibria, mass and energy balances, solvent and energy requirements, and heat- and mass-transfer rates, as a function of the key operating parameters (KOPs). The novelty of this work is that our approach collapses the what is otherwise a very large variable space to a reduced number of selected KPIs. Following this strategy, solvents can be evaluated given that their key properties have been fully determined or predicted.²³ Our results clearly indicate that, in addition to CO₂ capacity, the other solvent properties which have a primary effect on the price of the carbon capture are viscosity and heat capacity.

The remainder of this paper is structured as follows: Section 2 reviews the current state of the art of chemisorption for carbon capture. Section 3 presents the methodological and modelling approach developed in this study and the process model. Section 4 analyses the results of the effect of the characteristics of the solvent and the flue gas on the selected indicators. Finally, Section 5 presents the conclusions of our work.

2 Chemical solvents for carbon capture

Monoethanolamine (MEA) is a fast reacting alkanolamine, and was first proposed for gas separations by R. R. Bottoms in 1930,²⁴ and is generally used as the benchmark against which all other CO₂ capture processes are compared, having been proven at both pilot and commercial scales. The reaction between CO₂ and MEA involves the formation of a carbamate salt.²⁵ The stoichiometry of this reaction limits the loading capacity to 0.5 moles of CO₂ per mole of the amine.²⁶ The viscosity of its aqueous solution is similar to that of water.²⁷ However, it is a relatively volatile compound^{28,29} leading to partial vaporisation of the amine and subsequent release into the environment. Furthermore, large amounts of energy are required to break the stable carbamate bond (~85 kJ mol⁻¹)^{22,30,31} and desorb the CO₂ from the solvent. The total thermal energy requirements are estimated to be in the range of 3.5 to 4 GJ per tonne of CO₂, as a function of process configuration, and are composed of the contributions to the heat duty of regeneration: (i) the energy required to break the chemical bond between CO₂ and amine, (ii) the energy required to generate stripping steam in the reboiler and (iii) the sensible heat required to raise the temperature to that of the regeneration.^{22,32}

Secondary amines, *e.g.*, diethanolamine (DEA), and tertiary amines, *e.g.*, triethanolamine (TEA) and *N*-methyl-diethanolamine (MDEA), have also been investigated for carbon capture. Secondary and tertiary amines tend to have both a reduced rate of reaction and energy of regeneration. Sterically hindered compounds were first proposed by Sartori and Savage in 1983.³³ At that time, they were proposed as a means to increase the carrying capacity of the solvent above that of standard primary alkanolamines. The primary driver for this was the relatively low



inlet and outlet gas respectively, and n_i^{abs} is the rate of capture expressed as the mole flow rate.

The mass transfer has been modelled following the two-film theory⁶⁶ as reviewed for carbon capture by Wilcox *et al.*⁶⁷ Non-reactive thermodynamic equilibrium is assumed to be attained at the gas–liquid interface. If absorption occurs at low pressure, it can be assumed that it obeys Henry's law, so the molar fraction of the solute at the liquid interface with the physical solvent ($x_i^{0,I}$), assuming ideal gas and liquid, would be calculated as:

$$y_i^I = H_i x_i^{0,I} \quad (2)$$

where y_i^I is the molar fraction of the solute at the gas interface and H_i is Henry's coefficient. The mass transfer resistance is considered to occur in the vicinity of the gas–liquid interface or the fluid film. The liquid mass transfer coefficient (k_L) has been estimated using Onda's correlations for randomly packed columns:⁶⁸

$$k_L \left(\frac{\rho_L}{\mu_L g} \right)^{\frac{1}{3}} = 0.0051 \frac{\text{Re}^{2/3} (a_p d_p)^{0.4}}{\text{Sc}_L^{0.5}} \quad (3)$$

where Sc_L is the Schmidt number for the liquid phase, and Re_L is the Reynolds number using the wet interfacial area (a') calculated as a correction of the packing specific area (a_p) using Onda's correlation:

$$a' = a_p \left(1 - \exp \left(-1.45 \left(\frac{\sigma_c}{\sigma} \right)^{0.75} \text{Re}_L^{0.1} \text{Fr}_L^{-0.05} \text{We}_L^{0.2} \right) \right) \quad (4)$$

where σ is the surface tension of the liquid and σ_c is the critical surface tension of the packing. Fr_L and We_L are the Froude and Weber dimensionless numbers for the liquid phase.

The calculation of the rate of diffusion is ordinarily one of the most computationally intensive elements of an absorption model, typically employing a Maxwell–Stefan formulation. However, in the context of this study, such an approach would run counter to our aim of developing a high throughput screening tool. Thus we include a description of the limiting diffusivity, *i.e.*, the diffusion of the unreacted base to the reaction plane. Therefore, the diffusivity coefficient has been estimated using:

$$D_L = x_B D_{B,H_2O}^0 + x_{H_2O} D_{H_2O,B}^0 \quad (5)$$

where the diffusivity coefficients at infinite dilution were estimated with the Wilke–Chang correlation:⁶⁹

$$D_{ij}^0 = 7.4 \times 10^{-8} \frac{(\phi M_j)^{1/2} T}{\mu V_i^{0.6}} \quad (6)$$

where M_j is the molecular weight of solvent j , V_i is the molecular volume of the solute i , and ϕ is the association factor of the solvent. ϕ is chosen as 2.6 for water,⁶⁹ and 2.26 for the base.⁷⁰

The enhancement factor E is defined as the ratio of the average rate of absorption into an agitated liquid in the presence of the reaction to the average rate of absorption without the reaction. Kenig *et al.* discretised the film region and demonstrated that the chemical reaction occurring at the film considerably enhances the mass transfer of CO_2 within the film

region.⁷¹ In the cases where the reaction is instantaneous, the enhancement factor is only a function of the diffusion, and consequently, dividing the film into segments does not improve the result. Therefore, for these cases when the reaction is instantaneous, the enhancement factor can be estimated by:

$$E = 1 + \frac{D_B c_B}{z D_L c_{\text{CO}_2}^I} \quad (7)$$

where D_B is the diffusivity coefficient of the binder component in the aqueous phase, $c_{\text{CO}_2}^I$ is the molar concentration of CO_2 at the liquid interface, c_B is the molar concentration of the binder component, and D_L^i is the diffusion coefficient of component i in the liquid phase. For a fast pseudo-first order reaction, the enhancement factor can be estimated as:⁷²

$$E = \frac{\sqrt{D_L k_2 c_B}}{k_L} \quad (8)$$

where k_2 is the pseudo-first order reaction constant.

Dimensions of the column. The total number of moles N_{CO_2} absorbed or desorbed in the process column is calculated from the total contact area which is a function of the size of the tower and the type of packing:

$$N_{\text{CO}_2} = J_{\text{CO}_2} \varepsilon a' A_T Z_T \quad (9)$$

where ε is the void fraction of the packing, A_T is the cross-sectional area of the column and Z_T is the height of the absorber or desorber tower.

The molar flux of CO_2 at the interface J_{CO_2} can be therefore calculated using:

$$J_{\text{CO}_2} = k_L^0 E (c_{\text{CO}_2}^{0,I} - c_{\text{CO}_2}^B) \quad (10)$$

Considering that CO_2 reacts across the film, it is reasonable to assume that the concentration of molecular CO_2 in the bulk liquid is negligible.⁷¹ The 0 indicates that no chemical reaction is considered at the interface, and only physical absorption is occurring. For the fast pseudo-first order, the size of the column can be estimated combining eqn (8)–(10) giving:

$$N_{\text{CO}_2} = \sqrt{D_L k_2 c_B c_{\text{CO}_2}^{0,I}} \varepsilon a' A_T Z_T \quad (11)$$

This approach reduces the numerical complexity of the absorption model in order to permit the rapid evaluation of the performance of a sorbent, but still capturing the influence of the reaction kinetics, the mass transfer across the gas–liquid interface, the thermodynamic equilibrium and the hydrodynamics of the packing.

Energy balance equations. The absorber has been modelled as an adiabatic column,^{61,73} where the gas and the liquid transfer heat through the absorption of CO_2 and the vaporisation of water:

$$\Delta H^I = \Delta H^V - \sum_j n_j \Delta h_j^{I-g} \quad (12)$$

where h_j^{I-g} is the specific enthalpy of phase change, *e.g.*, the absorption or desorption of CO_2 and the heat of vaporisation of water, and ΔH^I and ΔH^V are the changes of enthalpy in the



liquid and vapour phase respectively, which are estimated using:

$$\Delta H^l = 0.5 \left(v^{\text{in}} C_p^{\text{L,in}} + v^{\text{out}} C_p^{\text{L,out}} \right) (T^{\text{in}} - T^{\text{out}}) \quad (13)$$

$$\Delta H^v = 0.5 \left(v^{\text{in}} C_p^{\text{v,in}} + v^{\text{out}} C_p^{\text{v,out}} \right) (T^{\text{v,in}} - T^{\text{v,out}}) \quad (14)$$

where C_p is the heat capacity at the corresponding temperature T of the inlet and outlet liquid and vapour streams.

Pilot plant experiments show that the temperature across the desorber height can be estimated as the average value between the temperatures of the lean solvent entering the absorber and the rich solvent leaving the absorber⁷⁴ and therefore, the stripper has been modelled as an isothermal system.⁷⁵

3.2 Thermodynamic modelling

The solubility of CO_2 in alkanolamines is calculated using the equilibrium model proposed by Gabrielsen *et al.*,⁷⁶ where the gas is considered ideal, and Henry's coefficient is combined with the chemical equilibrium constant:

$$P y_{\text{CO}_2} = K_{\text{CO}_2} x_{\text{CO}_2} \frac{\alpha_0 \theta}{(\alpha_0 (1 - z\theta))^2} \quad (15)$$

where P is the total pressure, α is the mole fraction of amine in the solution, θ is the CO_2 loading, z is the ratio of amine per mole of CO_2 (e.g., $z = 2$ for MEA) and K_{CO_2} is the combined Henry's law and chemical equilibrium. K_{CO_2} is estimated as a function of the temperature, the amine concentration and the loading:

$$\ln K_{\text{CO}_2} = A + \frac{B}{T} + C\alpha_0\theta + D\sqrt{\alpha_0\theta} \quad (16)$$

where A , B , C , and D are amine-specific parameters.⁷⁶ Following the approach described by Kale *et al.*,⁵⁷ Henry's law is used to describe the physical vapour-liquid equilibrium of CO_2 and N_2 at the interface. Henry's law constant of a solute in a blend solvent can be estimated from Henry's law constants of the solute in each of the pure solvents.⁷⁷ Henry's coefficient of reactive solvents is estimated using the so-called N_2O analogy, where dinitrogen monoxide (N_2O) is used as a non-reactive gas to estimate the properties of the gases in liquids such as diffusivity and solubility.^{78,79} The extended Raoult's law for MEA and water is applied to determine the vaporisation of both components into the gas stream using the activity coefficients reported by Park *et al.*⁸⁰

3.3 Heat exchangers

The process model includes two heat exchangers without phase change, *i.e.*, the lean-rich heat exchanger and the lean cooler, and two heat exchangers with phase change, *i.e.*, the condenser and the reboiler. In all cases they have been modelled as shell-and-tube units, with the condenser being considered to be the vertical condenser and the reboiler being modelled as a thermosiphon. The general equation for the heat transfer area is:

$$Q = UA_{\text{HE}}\Delta T_{\text{LM}} \quad (17)$$

where Q is the heat exchange rate, A_{HE} is the area of heat exchange, and ΔT_{LM} is the logarithmic mean temperature difference of the two streams exchanging heat. The overall heat transfer coefficient U is the reciprocal of the sum of the different heat transfer resistances. For a tube heat exchanger the overall heat transfer coefficient U is typically estimated as:

$$\frac{1}{U} = \frac{1}{h_i} + \frac{e_t}{k_w} + \frac{1}{h_o} + \frac{2}{h_d} \quad (18)$$

where h_i , h_o and h_d are the heat transfer coefficient of the fluid inside the tube, the heat transfer coefficient of the fluid outside the tubes (in the shell) and the heat transfer coefficient of the dirt, respectively. e_t is the thickness of the tube, and k_w is the thermal conductivity of the heat exchanger wall.

Single phase heat exchangers. The heat rate in a heat exchanger where no phase change occurs is given by the sensible heat:

$$Q = m \widehat{C}_p \Delta T \quad (19)$$

where m is the mass flow rate of the stream, ΔT is the temperature difference between the inlet and the outlet of the stream, and \widehat{C}_p is the arithmetic average heat capacity in the range ΔT .

The fluid heat transfer coefficient value depends on the flow regimes, which is a function of the heat exchanger internals and arrangements and on the fluid properties. For turbulent flow, the heat transfer coefficient for the inside fluid has been estimated *via*:

$$\text{Nu}_i = C \text{Re}_i^{0.8} \text{Pr}_i^{\frac{1}{3}} \left(\frac{\mu}{\mu_w} \right)^{0.14} \quad (20)$$

where $C = 0.023$ for non-viscous liquids and 0.027 for viscous solvents, Nu , Re and Pr are the dimensionless numbers of Nusselt, Reynolds and Prandtl respectively, which are calculated as:

$$\text{Nu} = \frac{h_i d_i}{k} \quad (21)$$

$$\text{Re} = \frac{u d_i \rho}{\mu} \quad (22)$$

$$\text{Pr} = \frac{C_p \mu}{k} \quad (23)$$

where d_i is the internal diameter of the tube, k is the thermal conductivity of the fluid, u is the linear velocity of the fluid, ρ is the density and μ and μ_w are the viscosity at the fluid temperature and at the wall temperature respectively.

The heat transfer coefficient of the shell side is calculated using Kern's method:⁸¹

$$\text{Nu}_o = j_h \text{Re}_o \text{Pr}_o^{\frac{1}{3}} \left(\frac{\mu}{\mu_w} \right)^{0.14} \quad (24)$$

where j_h is the shell-side factor. The value of j_h can be found elsewhere.⁸²



Two-phase heat exchangers. The heat rate in a phase change heat exchanger which is given by both the sensible heat and the latent heat:

$$Q = m\widehat{C}_p\Delta T + \sum_j m_j\Delta h_j^{l-g} \quad (25)$$

where m_j is the mass of component j that changes the phase, and Δh_j^{l-g} is the specific enthalpy of phase change, *e.g.*, the heat of vaporisation. The heat associated with the absorption or desorption of CO₂ might be included in this term if applicable. The condenser has been modelled as a horizontal exchanger with condensation in the shell. The heat transfer coefficient of the condensate (h_c) for a tube bundle is given by:⁸¹

$$h_c = 0.95\kappa_L \left[\frac{\rho_L(\rho_L - \rho_v)g}{\mu_L\Gamma_h} \right]^{1/3} \quad (26)$$

where g is the gravitational acceleration (9.81 m s⁻¹) and Γ_h is the condensate flow per unit length of tube. The condensate density (ρ_L), viscosity (μ_L) and thermal conductivity (κ_L) are evaluated at the mean of the temperature of condensation and the tube-wall temperature.

The reboiler has been modelled as a thermosiphon using the model proposed by Chen for forced-convective boiling.⁸³ This method considers that the heat transfer of the boiling stream is the sum of the contribution of convective and nucleate boiling. The convective boiling coefficient can be estimated using eqn (20) corrected by a two-phase flow factor based on the Lockhart–Martinelli two-phase flow parameter.⁸⁴ The nucleate boiling coefficient is estimated using the Forster and Zuber correlation.⁸⁵

3.4 Economic indices

A key objective of this work is to relate the cost of the carbon capture plant to the properties of the solvents. Our model uses the Total Annualised Cost (TAC) as the index against which to assess the economic performance of the plant:

$$\text{TAC} = \text{CRF} \sum_k^{\text{units}} \text{CAPEX}_k + \sum_l \text{OPEX}_l \quad (27)$$

where the CRF is the capital recovery factor and is given by

$$\text{CRF} = \frac{i(1+i)^n}{(1+i)^n - 1} \quad (28)$$

which is a function of the discount rate i and the annuity period n . A discount rate of 10% and an annuity period of 25 years have been assumed. The capital cost, CAPEX, for each unit has been estimated using correlations that link the cost to key properties of the unit, *e.g.*, the area of a heat exchanger, or the dimensions of the column.⁸⁶ For example, the installed cost§ of an absorption column and a heat exchanger is given by eqn (29) and (32), respectively.

$$C_{\text{abs}} = 1.281[f_1 C_b + V_p C_p + C_{p1}] C_I \quad (29)$$

where f_1 refers to the material of construction and is assigned a value of 2.1 for SS316¶ and C_b is a function of the weight of the shell, given by:

$$C_b = 1.218 \exp[6.629 + 0.1826(\ln W) + 0.02297(\ln W)^2] \quad (30)$$

where W is the weight of the shell. In this work, a thickness of 2 mm|| was assumed. The product $V_p C_p$ corresponds to the cost of column internals, where V_p is the volume of packing required and C_p is the specific cost of the packing used. V_p is directly calculated *via* the column sizing equations and C_p is assigned a value of \$76.6 ft⁻³, representative of the packing used in this study. Finally, C_{p1} is given by:

$$C_{p1} = 300D^{0.7396} Z_T^{0.7068} \quad (31)$$

where D and Z_T are the column diameter and tan-to-tan height, respectively.

In the case of heat exchangers,

$$C_{\text{HX}} = 1.218(f_d/f_m/f_p C_b) C_I \quad (32)$$

where f_d , f_m , and f_p are functions of the heat exchanger type, material of construction and pressure range, respectively. C_b is an explicit function of the heat transfer area, A , and is given by:

$$C_b = \exp[8.821 - 0.30863(\ln A) + 0.0681(\ln A)^2] \quad (33)$$

In both eqn (29) and (32), C_I is a cost multiplier to account for the cost of installation and is assigned the value 2.1 and 1.9 for stainless steel absorption columns and heat exchangers, respectively. More details on these equations and their derivation can be found in the work of Couper.⁸⁶

Thus, it is possible to make a direct connection with solvent thermophysical or kinetic properties and system cost. For example, the viscosity of the solvent influences the diffusivity (eqn (5) and (6)) which, in turn influences the flux (eqn (10)) and the height of the column (eqn (11)). Finally, this dictates the installed cost of the absorber (eqn (29)) and thus the TAC of the entire system (eqn (27)). A thorough evaluation of the sensitivity of key process design variables and TAC to solvent properties is presented in Section 4.

The cost derived from the electricity consumption and from the heat requirements has been estimated separately. The short-run marginal cost (SRMC) of the electricity has been used assuming a price of coal of \$50 per t_{coal},⁸⁷ and the price per tonne of CO₂ emitted is \$70 per t_{CO₂}.⁸⁸ The cost of steam has been estimated using the SRMC assuming that the efficiency of the boiler is 90%. The annualised costs, *i.e.*, annual CAPEX, OPEX and TAC, are then divided by the tonnes of CO₂ captured in one year. The costs of compression of the CO₂ for transport and storage have not been included in this work. A previous study shows that the cost of CO₂ compression and dehydration is on the order of \$20–25 per t_{CO₂}.⁸⁹

¶ This value can range between 1.7 for carbon steel and up to 7.7 for titanium.

|| This value could be increased if a more corrosive solvent were to be used.

§ All costs are calculated in 2010 USD.



4 Results and discussion

This section has been structured as follows: we first investigate the effect of a range of thermo-physical and chemical properties of the solvents on selected monetised and non-monetised indices. The minimum set of properties required for solvent evaluation using our methodology are thermodynamic equilibria of CO₂, reaction constant(s), viscosity, density, heat capacity, thermal conductivity and surface tension. For this, we evaluate a carbon capture plant treating 900 kg s⁻¹ of flue gas containing 12% (v/v) of CO₂ from an 800 MW supercritical pulverised coal power plant (ScPC). We assume that the plant runs for 335 days per year at 100% capacity. The capture rate is set to 90% of the carbon emitted by the power plant. We aim to identify and rank these thermophysical properties that have the most prominent impact on the cost of the capture plant. Then, we explore the trade-offs that these properties have on the monetised indices *via* a comprehensive sensitivity analysis.

Next, we examine in more detail the CO₂ transport from the gas phase into the liquid in the absorber by analysing the effect of thermodynamics, reaction kinetics and transport properties on the molar flux across the interface. Furthermore, we study the effect of the concentration of CO₂ in the gas phase by analysing how the flux is affected when the flue gas treated comes from a ScPC plant and from a combined cycle gas turbine (CCGT). The concentration of CO₂ in the CCGT is assumed to be 4% (v/v). Finally, we compare the process performance of the carbon plant dedicated to treat the flue gas from that of a ScPC with that of CCGT considering the same net power output for both power plants.

We have selected 30 wt% MEA as the benchmark solvent. Table 1 shows its properties at 303 K. Our model assumes that the coefficient between the new value and that of the benchmark is constant across the temperature range studied. That is, if the property doubles at 303 K with respect to the benchmark, it also doubles at 393 K. We have fixed the rich loading to 0.47 and the lean loading to 0.3. The results show that the TAC of the capture process is \$51 per t_{CO₂}, which gives a total cost of the CO₂ capture of \$73 per t_{CO₂} once the costs of CO₂ compression and dehydration are accounted for.⁸⁹ This is in line with current projections of the cost of carbon capture on an industrial scale,⁹⁰ for example, the Petra Nova Carbon Capture Project, whose cost has been estimated to be \$70 per t_{CO₂}.⁹¹

Table 1 Properties of 30% aqueous solution of MEA at 303 K

Property	Value
Equilibrium constant (kPa)	0.015
Henry's coefficient (kPa m ⁻³ kmol ⁻¹)	4560
Reaction constant (m ³ kmol ⁻¹ s ⁻¹)	8008
Density (kg m ⁻³)	1168
Viscosity (mPa s)	2.51
Heat capacity (kJ kmol ⁻¹ s ⁻¹)	89.7
Thermal conductivity (kJ m ⁻¹ s ⁻¹ K ⁻¹)	4.75 × 10 ⁻⁴

4.1 Evaluation of the thermophysical properties of solvents

Using our modelling tool, we have identified the following properties that can affect the process performance of the carbon capture: density, viscosity, surface tension, heat capacity, thermal conductivity, heat of absorption which might inherently include the heat of reaction in the case of reactant solvents, and CO₂ solubility, which might be expressed in terms of loading, Henry's coefficient or a generic equilibrium constant. A sensitivity analysis has been carried out to determine the aftermaths of varying each of the aforementioned properties on the annualised CAPEX, OPEX and TAC of the carbon capture plant. Every property has been screened individually by varying its value within sensible ranges that were selected based on typical values of solvents.

Equilibrium constant. The equilibrium constant of the CO₂-amine-H₂O system is the main thermodynamic property of the system. It is a non-linear function of the temperature, the partial pressure of CO₂, the concentration species in the mixture and Henry's coefficient of CO₂ in the liquid phase. The latter is related to the theoretical physical solubility in the solvent if no reaction would take place between the CO₂ and the solvent components. Note that the equilibrium constant and Henry's coefficient are inverse functions of the gas solubility. For decades, the search of a more effective solvent for carbon capture has been largely driven by improving the value of the equilibrium constant. A more CO₂-philic solvent reduces the solvent flow rate, the size of the units and the heat requirements which are related to the sensible heat. Fig. 2 illustrates the increase in size of the absorption column when the equilibrium constant (see eqn (16)) increases, *i.e.*, the solubility of CO₂ decreases. The cost associated with the change of the equilibrium constant is shown in Fig. 3. At higher equilibrium constant, the CO₂ has a lower tendency to stay in the liquid phase. This has an opposite effect in the CAPEX and in the OPEX. The size of the process units increases as shown in Fig. 2, increasing the capital cost. However, a lower solubility, *i.e.*, a weaker solvent, facilitates the recovery of the solvent, and therefore reducing the heat requirements in the reboiler.⁹² This is in accordance with the van't Hoff equation, which can be

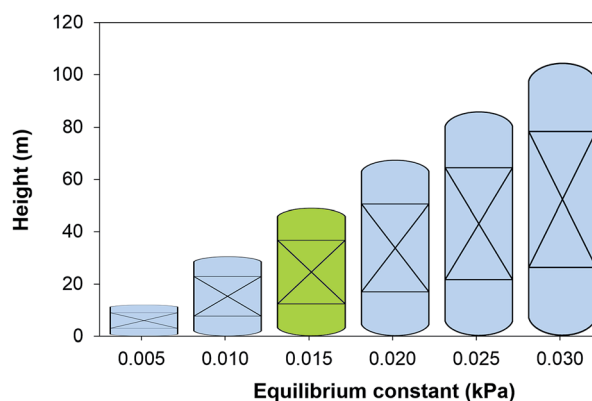


Fig. 2 Height of the absorber as a function of the chemical equilibrium constant of the solvent at 303 K. Green figure corresponds to the height of an absorber using 30 wt% MEA.



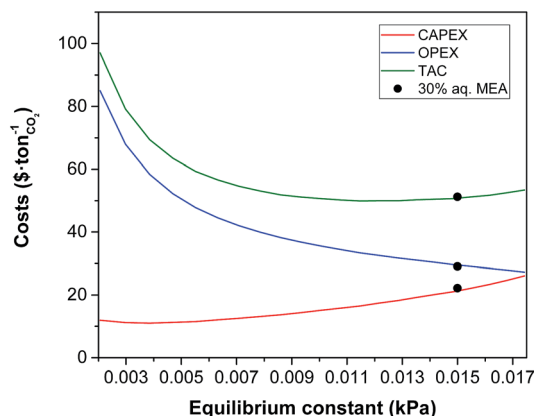


Fig. 3 Effect of equilibrium constant of CO₂ in the solvent on the annualised CAPEX, the OPEX and the TAC of the carbon capture plant.

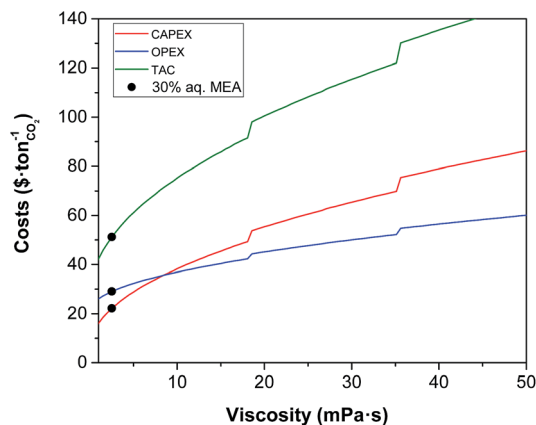


Fig. 5 Effect of viscosity on the annualised CAPEX, the OPEX and the TAC of the carbon capture plant.

derived from the Gibbs-Helmholtz equation, where the enthalpy of solution of a gas in a solute is related to the equilibrium constant.³² An increase in the CO₂ capacity, *i.e.*, lower equilibrium constant, results in larger enthalpies of solutions for strong chemical solvents, as discussed in the work of Mathias and O'Connell.⁹³

Viscosity. The impact of the viscosity of the solvent on the absorber height is illustrated in Fig. 4, and on the annualised CAPEX, the OPEX and the TAC is shown in Fig. 5. For reference, the viscosity of a 30 wt% MEA solvent at 313 K is 2.5 mPa s.²⁷ If a solvent presents a viscosity of 16 mPa s, the total cost of the equipment is estimated to be more than double that of the benchmark plant. At this viscosity, the height of the absorber required is 133 m, as seen in Fig. 4, compared to the 50 m absorber required for the benchmark viscosity. The viscosity has a significant impact on the hydrodynamics of the absorber, particularly on the hold-up.⁹⁴ The mass transfer of the gas in the liquid phase is hindered at higher viscosities. Therefore, longer contact times are required to achieve the same degree of separation, resulting in taller towers. Furthermore, heat exchangers are greatly affected by the viscosity, with a larger impact on

these units which work at lower temperatures, *e.g.*, the lean cooler, wherein even moderate viscosities result in low Reynolds numbers. At higher viscosities, the flow in the tubes develops from turbulent to laminar regimes, changing radically the hydrodynamics and the heat transfer performance. In the case of the turbulent regime, the fluid flow obviously advances in the axial direction across the tube, but additionally, it is constantly undergoing multidirectional swirling and mixing. As a consequence, the liquid surface in contact with the tube walls is continuously renewed. The convective contribution to the heat transfer prevails over the conductive contribution, enhancing the heat transfer in these systems. In contrast, in the case of laminar flow, the fluid only flows in the axial direction in parallel layers which do not mix. Thus, conduction is the leading mechanism for heat transfer. The effect of the regime transition from turbulent to laminar on the cost of the process is illustrated in Fig. 5. The discontinuities in the costs correspond to the viscosities at which the flow regime experiences this transition in the cooler (18 mPa s) and the heat exchanger (36 mPa s). The annualised CAPEX increases from \$48 per t_{CO₂} to \$54 per t_{CO₂} as a result of the transition from turbulent to laminar flow in the cooler, *i.e.*, the CAPEX increases by 12.5%.

Higher values of viscosity increase pump power as a result of changes in the hydraulic behaviour of the solvent associated with a higher friction factor and pressure drop, thus increasing the operational challenges. Yang *et al.* reported that a mixture of aqueous MEA with an ionic liquid blocked the pipelines and their pumps stopped operating when they used a mixture with a viscosity of 16 mPa s.⁹⁵ However, the cost related to the electric requirements represents 5% of the total OPEX of the process. Thus, an increase in plant electricity requirements does not correspond to a significant increase in process costs. The results show that the cost of the electric requirements is \$1 per t_{CO₂} at the viscosity of the benchmark, whereas at 40 mPa s the cost is \$2.7 per t_{CO₂} relative to an operating cost of \$56 per t_{CO₂} at this viscosity; a negligible amount.

Heat capacity. The heat capacity is the only property that has a pronounced effect on both the CAPEX and the OPEX as illustrated in Fig. 6. As a reference, the heat capacity of 30%

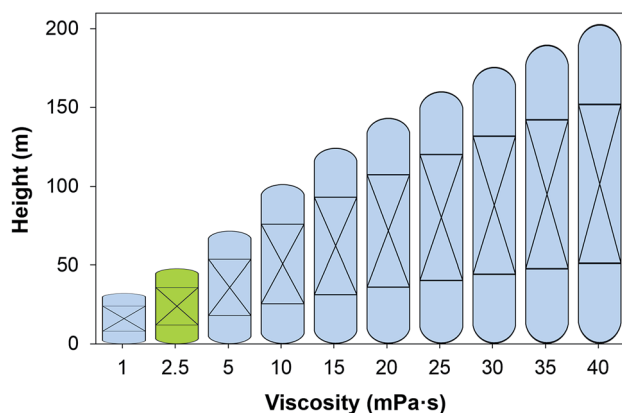


Fig. 4 Height of the absorber as a function of the viscosity of the solvent at 303 K. Green figure corresponds to the height of an absorber using 30 wt% MEA.





Fig. 6 Effect of heat capacity of the solvent on the annualised CAPEX, the OPEX and the TAC of the carbon capture plant.

MEA in water at 303 K is $89 \text{ kJ kmol}^{-1} \text{ K}^{-1}$ or $3.6 \text{ kJ kg}^{-1} \text{ K}^{-1}$. The increase in the TAC with the heat capacity is obvious. Higher values of heat capacity of the solvent result in higher heating and cooling requirements, *i.e.*, in the OPEX. As a result, larger contact areas are required in the heat exchangers, upon increasing the CAPEX. Conversely, the overall heat transfer coefficient increases with the heat capacity. However, this increase is minor, and its contribution towards the reduction of the CAPEX is negligible compared to the increase driven by a larger area. Less evident is, though, the increase of CAPEX at low values of heat capacity. At lower heat capacity, the temperature of the solvent further increases as it moves downward the absorber given the same enthalpy of the reaction. The capacity of the solvent to absorb CO_2 declines with temperature. Therefore, the rich loading of the solvent decreases, requiring more solvent to capture the same amount of CO_2 . This leads ultimately to larger units, and consequently to higher CAPEX.

Density. Density has a limited impact on the CAPEX and a minor effect on the OPEX, as shown in Fig. 7. The fact that it is the only property that decreases the cost as it increases is noteworthy. For example, if there was a solvent with a density double that of water, it would reduce the unit cost by 20%.



Fig. 7 Effect of the density of the solvent on the annualised CAPEX, the OPEX and the TAC of the carbon capture plant.

Thermal conductivity and surface tension. We found that varying the thermal conductivity and the surface tension of the solvents has a minor effect on the overall cost of the carbon capture plant compared to the effect of the properties investigated above. Having said that, the surface tension is expected to play a more important role in the case of non-reactive solvents.⁶⁷ In conclusion, viscosity and heat capacity are the primary thermophysical properties that together with the equilibrium constant impact the mass transfer and the energy transfer. The feasible parameter space which corresponds to a reduction in the cost of carbon capture with respect to the benchmark is identified in Fig. 8. It is clear that any potential solvent for carbon capture should not only improve the CO_2 carrying capacity, but also present a reduced value of viscosity and heat capacity and an increased density with respect to those of the benchmark. Nevertheless, these properties cannot be tuned independently from each other as they are a function of the chemical structure and its functional groups. Therefore, any molecular design of prospective candidate molecules should take this into account. Functionalising the molecular structure intending to improve the CO_2 carrying capacity might counteract the aim of reducing the cost of carbon capture. For example, increased functionalization (increasing carrying capacity) might also increase viscosity.

In the next sections we explore the trade-offs between the viscosity, the equilibrium constant and the heat capacity. Frequently, the effort to design solvents with a higher CO_2 leads to chemical structures that contain atoms or functional groups that not only interact more efficiently with the CO_2 but also present intra- or intermolecular interactions, increasing the viscosity of the system. Fig. 9 shows the effect of both properties on the monetised indices of the process. The effect of the viscosity in the flow regime inside the heat exchanger discussed above (see Fig. 5) is captured again in Fig. 9.

The discontinuity of the evolution of the CAPEX with the viscosity corresponds to the points where the flux transitions from turbulent to laminar in the heat exchangers. Interestingly, the heat capacity can displace the laminar regime front towards



Fig. 8 Relative effect on the TAC as a function of the relative density, viscosity, heat capacity and equilibrium constant with respect to the same properties and the cost of the capture plant using the benchmark solvent, *i.e.*, 30% MEA.



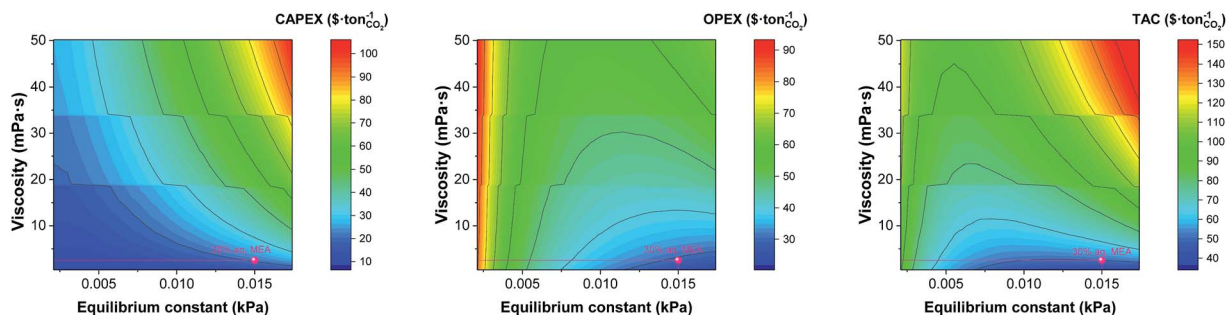


Fig. 9 Trade-offs between the equilibrium constant and the viscosity on annualised CAPEX, OPEX and TAC. The value represented here correspond to that at the top of the absorber, *i.e.*, 303 K.

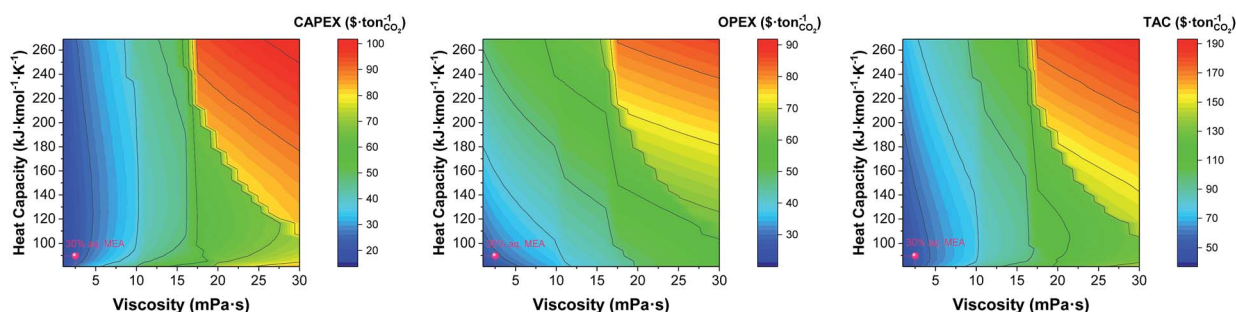


Fig. 10 Trade-offs between the viscosity and the heat capacity of the solvent on annualised CAPEX, OPEX and TAC. The value represented here correspond to that at the top of the absorber, *i.e.*, 303 K.

lower viscosities, as shown in Fig. 10. At the heat capacity of the benchmark, the first transit to laminar flow in the cooler occurs at viscosities 7 times higher than the viscosity of the benchmark. When the heat capacity doubles, the laminar front is found at 4.5 times the viscosity of the benchmark. This is an important observation as the heat capacity is usually overlooked in the screening, selection and design of solvents for carbon capture.

4.2 The competition between equilibrium, transport and kinetic properties

The absorption column might be considered the core of the capture process. Thus, solvent selection is particularly important here. A solvent with high CO₂ capacity per unit volume will serve to reduce the amount of solvent required, reducing both the CAPEX and the OPEX. Moreover, the foregoing results emphasise the importance of maximising rates of mass transfer in order to reduce the size and capital cost associated with the absorption column. Gas-liquid interphase mass transfer is a complex function of simultaneous transport and thermodynamic driven phenomena occurring across and at both sides of the interface. This includes the transport of the CO₂ through the gas-liquid interface, and then its diffusion entangled with the chemical reaction towards the bulk liquid. Understanding the contribution of the different parameters that determine the rate at which CO₂ is transferred from the gas to the liquid phase is imperative for the design of new solvents.⁶⁷ Fig. 11 shows the contrasting impact of diffusivity (D) and reaction constant (k_2)

for five different archetypal solvents with Henry's coefficients of 1000, 3000, 5000, 8000 and 10 000 kPa m³ kmol⁻¹, for an exhaust gas of 12 mol% (left) and 4 mol% (right) respectively. Note that by definition, Henry's coefficient and gas solubility are inversely related. Solvents with particularly high CO₂ solubility are represented by $H = 1000$ kPa m³ kmol⁻¹, whereas low CO₂ solubility solvents usually present Henry's coefficient values higher than 10⁴ kPa m³ kmol⁻¹. In the case of the high gas-phase CO₂ concentration, it is evident that liquid phase diffusivity is the rate limiting step in the absorption of CO₂, with reaction kinetics playing a secondary role. This is in line with previous results,⁹⁶ and reinforces the typical approximation of treating chemical reactions in these systems as equilibrium, as opposed to using a full reaction kinetic description. However, if a solvent has a lower CO₂ solubility, then the influence of diffusivity and reaction rate is of the same order. To illustrate this, let us perform the following thought experiment with two solvents, solvent A with Henry's coefficient of 3000 kPa m³ kmol⁻¹, and a solvent B with a significant higher CO₂ solubility exemplified in Fig. 10 by Henry's coefficient of 1000 kPa m³ kmol⁻¹. Let us assume that solvent A presents a high diffusivity, *e.g.*, 10⁻⁸ m² s⁻¹, and solvent B, which presents a markedly higher CO₂ solubility, has a hindered diffusivity coefficient below 10⁻⁹ m² s⁻¹. Solvent A outperforms the CO₂ flux of solvent B by 154% despite the lower CO₂ capacity because of its favoured transport properties.

Effect of the CO₂ concentration in the flue gas. Thus far, we have considered the performance of solvents in the context of



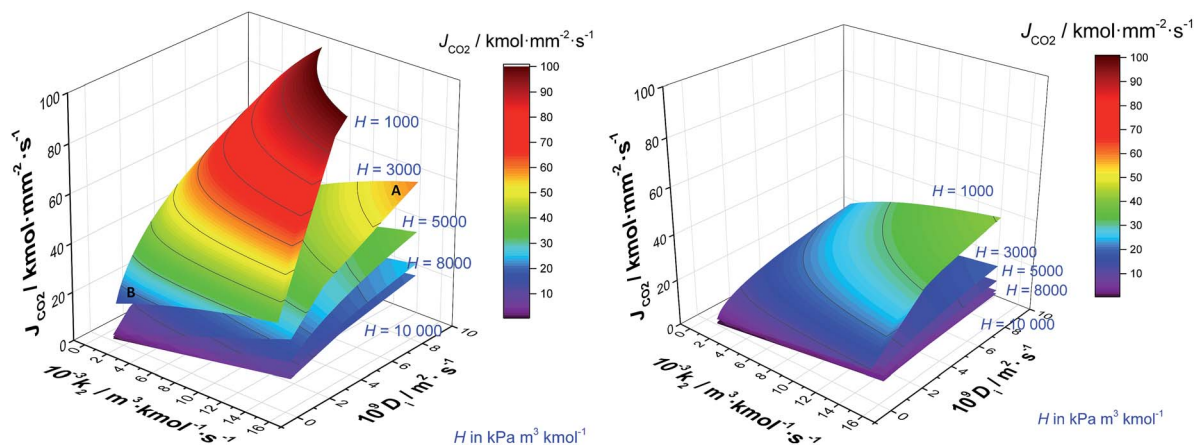


Fig. 11 CO_2 flux (J_{CO_2}) from ScPC flue gas (left) and from CCGT flue gas (right) to a solvent as a function of the diffusivity (D) and the pseudo-first order reaction (k_2) at five Henry's coefficient values, viz. 1000, 3000, 5000, 8000 and 10 000 $\text{kPa m}^3 \text{ kmol}^{-1}$ at 303 K and 0.1 MPa.

an exhaust gas with a relatively high CO_2 concentration, e.g., a coal fired power plant. However, it is increasingly recognised that it will also be necessary to capture CO_2 from dilute sources, such as the exhausts arising from gas-fired power stations. Therefore, in this section, we investigate how a low concentration exhaust gas, representative of that of a combined cycle gas turbine (CCGT), will affect the design of the carbon capture plant. Natural gas has a significantly higher hydrogen/carbon ratio, and thus the energy density of natural gas is higher than coal. Consequently, the carbon intensity of CCGT is significantly lower. The emission from coal ranges between 0.825 and 1.035 tons of CO_2 per MWh, whereas emissions from natural gas are in the range of 0.35–0.4 tons of CO_2 per MWh.⁹⁷

The typical flue gas from a coal plant contains 10–15% (v/v) of CO_2 , whereas the content of CO_2 of the flue gas from a gas plant is 3–5% (v/v). The impact that this much more dilute exhaust gas has on solvent performance is illustrated in Fig 10b. In this context, the dominance of Henry's constant and liquid phase diffusivity on the rate of CO_2 absorption is effectively eliminated. Here, each of CO_2 solubility, diffusivity and chemical kinetics plays approximately equivalent roles. This implies that retaining the kinetics in sorbent screening is important and that treating these reactions as equilibrium is likely to be a poor approximation.

5 Conclusions

We have presented a process performance indexed methodology to assess the potential of chemical solvents for carbon capture. Monetised (e.g., CAPEX, OPEX and TAC) and non-monetised (e.g., equipment size) KPIs are evaluated as a function of the selected KOPs of the process and the characteristics of the solvent. The KOPs include the solvent flow rate as a function of the exhaust gas composition, the rate of absorption and the SRMC of the steam available. The characteristics of the solvent are the kinetics of the reaction, the thermodynamic, and physico-chemical properties and the transport properties of the solvent, i.e., reaction constant, equilibrium constant, heat of reaction, molecular weight, density, heat capacity, viscosity, thermal conductivity and surface tension

of the solvent. Historically, most effort on solvent development has focused on enhancing the CO_2 absorption and reducing the heat of reaction, neglecting the effect of other properties on the process cost, particularly on the capital cost contribution to the overall cost of CO_2 capture (\$ per t_{CO_2}). The properties that have a primary importance for the TAC of CO_2 capture are, in order of prominence:

- (1) Viscosity
- (2) Equilibrium loading of CO_2
- (3) Reaction kinetics
- (4) Heat capacity
- (5) Heat of absorption
- (6) Density
- (7) Surface tension

It must be recognised that, of these, the first three properties are significantly more important than the other four. The fact that solvent viscosity is found to be of primary importance confirms our hypothesis that, in order to rationally screen, select and design sorbents for chemical processes in general, and CO_2 capture in particular, a whole system approach is necessary. Otherwise, it is impossible to fully appreciate the impact of solvent thermophysical properties on process performance and therefore costs. The absence of such an approach to date has led to an over emphasis of CO_2 solubility in solvent selection and design, potentially limiting progress in this area. One of the main drawbacks to a “designer solvent” approach is the impact of solvent functionalisation on physical properties, or the unintended consequences that may accompany a sole emphasis on CO_2 capacity. Greater chemical functionalisation of molecular liquids almost inevitably leads to a rapid increase in viscosity, and a concomitant decrease in thermal and chemical stabilities. While the density of functionalised solvents is normally higher, our model identifies this as a minor impact, and is likely offset by the inevitable increase in heat of absorption and therefore regeneration energy. Our model clearly demonstrates that this creates an ever greater pressure on increased solubility to offset the reduced mass transport, thereby leading to a “death spiral” of offsetting



improvements in one property at the expense of another. Only a systematic approach to solvent design, with all properties appropriately weighted, can lead to an optimal (or possibly even improved) solvent design.

Conflicts of interest

There are no conflicts to declare.

Acknowledgements

The authors thank the United Kingdom Carbon Capture and Storage Research Council (UKCCSRC) (Grant No. UKCCSRC-199) for funding this work. The authors are grateful to P. Brandl for proof reading the manuscript and assistance with figures.

References

- 1 IPCC, *Climate Change 2014: Mitigation of Climate Change: Contribution of Working Group III to the Fifth Assessment Report of the Intergovernmental Panel on*, Cambridge University Press, 2014, p. 1132.
- 2 *The Global Status of CCS*, Summary report, 2016, <https://www.globalccsinstitute.com/publications/global-status-ccs-2016-summary-report>.
- 3 Global CCS Institute, *Large Scale CCS Projects*, 2017, <https://goo.gl/Wv0Vvk7>.
- 4 *Cost and Performance of Carbon Dioxide Capture from Power Generation*, IEA technical report, 2011.
- 5 *Carbon Capture & Storage: Assessing the Economics*, McKinsey climate change initiative technical report, 2008.
- 6 R. Oxburgh, *Lowest Cost Decarbonisation for the UK: The Critical Role of CCS. Report to the Secretary of State for Business, Energy and Industrial Strategy from the Parliamentary Advisory Group on Carbon Capture and Storage*, 2016, <https://goo.gl/Afoyih>.
- 7 L. A. Hackett, *Commercialisation of CCS – What needs to happen?*, 2016, <https://tinyurl.com/y7mxxsu8>.
- 8 A. Samanta, A. Zhao, G. K. H. Shimizu, P. Sarkar and R. Gupta, *Ind. Eng. Chem. Res.*, 2012, **51**, 1438–1463.
- 9 J. Wang, L. Huang, R. Yang, Z. Zhang, J. Wu, Y. Gao, Q. Wang, D. O'Hare and Z. Zhong, *Energy Environ. Sci.*, 2014, **7**, 3478–3518.
- 10 R. Ben-Mansour, M. A. Habib, O. E. Bamidele, M. Basha, N. A. A. Qasem, A. Peedikakkal, T. Laoui and M. Ali, *Appl. Energy*, 2016, **161**, 225–255.
- 11 A. E. Creamer and B. Gao, *Environ. Sci. Technol.*, 2016, **50**, 7276–7289.
- 12 D. Clodic, R. El Hitti, M. Younes, A. Bill and F. Casier, *4th Annual Conference on Carbon Capture & Sequestration*, 2005, pp. 2–5.
- 13 M. J. Tuinier, M. van Sint Annaland, G. J. Kramer and J. A. M. Kuipers, *Chem. Eng. Sci.*, 2010, **65**, 114–119.
- 14 E. J. Anthony, *Ind. Eng. Chem. Res.*, 2008, **47**, 1747–1754.
- 15 I. Martínez, R. Murillo, G. Grasa and J. Carlos Abanades, *AIChE J.*, 2011, **57**, 2599–2607.
- 16 J. Adanez, A. Abad, F. Garcia-Labiano, P. Gayan and L. F. de Diego, *Prog. Energy Combust. Sci.*, 2012, **38**, 215–282.
- 17 P. S. Fennell and B. Anthony, *Calcium and Chemical Looping Technology for Power Generation and Carbon Dioxide (CO₂) Capture*, Elsevier Ltd., 2015.
- 18 R. Khalilpour, K. Mumford, H. Zhai, A. Abbas, G. Stevens and E. S. Rubin, *J. Cleaner Prod.*, 2015, **103**, 286–300.
- 19 N. Mac Dowell, N. Florin, A. Buchard, J. Hallett, A. Galindo, G. Jackson, C. S. Adjiman, C. K. Williams, N. Shah and P. Fennell, *Energy Environ. Sci.*, 2010, **3**, 1645–1669.
- 20 M. E. Boot-Handford, J. C. Abanades, E. J. Anthony, M. J. Blunt, S. Brandani, N. Mac Dowell, J. R. Fernández, M.-C. M.-C. Ferrari, R. Gross, J. P. Hallett, R. S. Haszeldine, P. Heptonstall, A. Lyngfelt, Z. Makuch, E. Mangano, R. T. J. Porter, M. Pourkashanian, G. T. Rochelle, N. Shah, J. G. Yao and P. S. Fennell, *Energy Environ. Sci.*, 2014, **7**, 130–189.
- 21 J. C. Abanades, B. Arias, A. Lyngfelt, T. Mattisson, D. E. Wiley, H. Li, M. T. Ho, E. Mangano and S. Brandani, *Int. J. Greenhouse Gas Control*, 2015, **40**, 126–166.
- 22 J. Oexmann and A. Kather, *Int. J. Greenhouse Gas Control*, 2010, **4**, 36–43.
- 23 A. Chremos, E. Forte, V. Papaioannou, A. Galindo, G. Jackson and C. S. Adjiman, *Fluid Phase Equilib.*, 2016, **407**, 280–297.
- 24 R. R. Bottoms, *US Pat.*, application 1783901, 1930.
- 25 P. M. M. Blauwhoff, G. F. Versteeg and W. P. M. Van Swaaij, *Chem. Eng. Sci.*, 1984, **39**, 207–225.
- 26 F.-Y. Jou, A. E. Mather and F. D. Otto, *Can. J. Chem. Eng.*, 1995, **73**, 140–147.
- 27 T. G. Amundsen, L. E. Øi and D. A. Eimer, *J. Chem. Eng. Data*, 2009, **54**, 3096–3100.
- 28 A. Belabbaci, A. Razzouk, I. Mokbel, J. Jose and L. Negadi, *J. Chem. Eng. Data*, 2009, **54**, 2312–2316.
- 29 K. Klepáčová, P. J. G. Huttenhuis, P. W. J. Derks and G. F. Versteeg, *J. Chem. Eng. Data*, 2011, **56**, 2242–2248.
- 30 I. Kim and H. F. Svendsen, *Ind. Eng. Chem. Res.*, 2007, **46**, 5803–5809.
- 31 Y. E. Kim, J. A. Lim, S. K. Jeong, Y. I. Yoon, S. T. Bae and S. C. Nam, *Bull. Korean Chem. Soc.*, 2013, **34**, 783–787.
- 32 I. Kim, K. A. Hoff, E. T. Hessen, T. Haug-Warberg and H. F. Svendsen, *Chem. Eng. Sci.*, 2009, **64**, 2027–2038.
- 33 G. Sartori and D. W. Savage, *Ind. Eng. Chem. Fundam.*, 1983, **22**, 239–249.
- 34 P. Singh, J. P. M. Niederer and G. F. Versteeg, *Int. J. Greenhouse Gas Control*, 2007, **1**, 5–10.
- 35 P. Singh, J. P. Niederer and G. F. Versteeg, *Chem. Eng. Res. Des.*, 2009, **87**, 135–144.
- 36 P. Singh and G. F. Versteeg, *Process Saf. Environ. Prot.*, 2008, **86**, 347–359.
- 37 G. Puxty, R. Rowland, A. Allport, Q. Yang, M. Bown, R. Burns, M. Maeder and M. Attalla, *Environ. Sci. Technol.*, 2009, **43**, 6427–6433.
- 38 D. Bonenfant, M. Mimeault and R. Hausler, *Ind. Eng. Chem. Res.*, 2003, **42**, 3179–3184.
- 39 S. Bishnoi and G. T. Rochelle, *Chem. Eng. Sci.*, 2000, **55**, 5531–5543.
- 40 T. Charkravarty, *Chem. Eng. Prog.*, 1985, **81**, 32–36.



- 41 H. Bosch, G. F. Versteeg and W. P. M. Van Swaaij, *Chem. Eng. Sci.*, 1989, **44**, 2745–2750.
- 42 D. A. Glasscock, J. E. Critchfield and G. T. Rochelle, *Chem. Eng. Sci.*, 1991, **46**, 2829–2845.
- 43 M. S. DuPart, P. C. Rooney and T. R. Bacon, *Hydrocarbon Process.*, 1999, **78**(4), 81–86.
- 44 L. Raynal, P. Alix, P. A. Bouillon, A. Gomez, M. Le Febvre De Nailly, M. Jacquin, J. Kittel, A. Di Lella, P. Mougin and J. Trapy, *Energy Procedia*, 2011, 779–786.
- 45 U. Liebenthal, D. D. D. Pinto, J. G. M.-S. Monteiro, H. F. Svendsen and A. Kather, *Energy Procedia*, 2013, **37**, 1844–1854.
- 46 S. Want and Z. Xu, in *Absorption-Based Post-Combustion Capture of Carbon Dioxide*, ed. P. Feron, Elsevier Science, 2016.
- 47 O. Aschenbrenner and P. Styring, *Energy Environ. Sci.*, 2010, **3**, 1106–1113.
- 48 M. Ramdin, T. W. de Loos and T. J. H. Vlugt, *Ind. Eng. Chem. Res.*, 2012, **51**, 8149–8177.
- 49 E. D. Bates, R. D. Mayton, I. Ntai and J. H. Davis, *J. Am. Chem. Soc.*, 2002, **124**, 926–927.
- 50 M. T. Mota-Martinez, M. Althuluth, M. C. Kroon and C. J. Peters, *Fluid Phase Equilib.*, 2012, **332**, 35–39.
- 51 L. F. Zubeir, M. H. M. Lacroix and M. C. Kroon, *J. Phys. Chem. B*, 2014, **118**, 14429–14441.
- 52 D. Shaw, *Energy Procedia*, 2009, **1**, 237–246.
- 53 D. G. Chapel, C. L. Mariz and J. Ernest, *Canadian Society of Chemical Engineers Annual Meeting*, 1999.
- 54 Y. Yagi, T. Mimura, T. Yonekawa and R. Yoshiyama, *GHGT-8*, 2006.
- 55 S. Holton, *Eight Annual Conferences on Carbon Capture and Sequestration*, 1999.
- 56 N. Asprion, *Ind. Eng. Chem. Res.*, 2006, **45**, 2054–2069.
- 57 C. Kale, A. Górak and H. Schoenmakers, *Int. J. Greenhouse Gas Control*, 2013, **17**, 294–308.
- 58 N. Mac Dowell, N. J. Samsatli and N. Shah, *Int. J. Greenhouse Gas Control*, 2013, **12**, 247–258.
- 59 N. Mac Dowell and N. Shah, *Int. J. Greenhouse Gas Control*, 2014, **27**, 103–119.
- 60 A. Lawal, M. Wang, P. Stephenson and H. Yeung, *Fuel*, 2009, **88**, 2455–2462.
- 61 R. E. Treybal, *Ind. Eng. Chem.*, 1969, **61**, 36–41.
- 62 H. M. Feintuch and R. E. Treybal, *Ind. Eng. Chem. Process Des. Dev.*, 1978, **17**, 505–513.
- 63 R. Krishnamurthy and R. Taylor, *AIChE J.*, 1985, **31**, 449–456.
- 64 R. Krishnamurthy and R. Taylor, *AIChE J.*, 1985, **31**, 456–465.
- 65 E. Y. Kenig, R. Schneider and A. Górak, *Chem. Eng. Sci.*, 2001, **56**, 343–350.
- 66 W. K. Lewis and W. G. Whitman, *Ind. Eng. Chem.*, 1924, **16**, 1215–1220.
- 67 J. Wilcox, P. Rochana, A. Kirchofer, G. Glatz and J. He, *Energy Environ. Sci.*, 2014, **7**, 1769.
- 68 K. Onda, H. Takeuchi and Y. Okumoto, *J. Chem. Eng. Jpn.*, 1968, **1**, 56–62.
- 69 C. R. Wilke and P. Chang, *AIChE J.*, 1955, **1**, 264–270.
- 70 E. D. Snijder, M. J. M. te Riele, G. F. Versteeg and W. P. M. van Swaaij, *J. Chem. Eng. Data*, 1993, **38**, 475–480.
- 71 E. Kenig, R. Schneider and A. Górak, *Chem. Eng. Sci.*, 1999, **54**, 5195–5203.
- 72 D. W. van Krevelen and P. J. Hoftijzer, *Chem. Eng. Prog.*, 1948, **44**, 529–536.
- 73 J. Pandya, *Chem. Eng. Commun.*, 1983, **19**, 343–361.
- 74 F. A. Tobiesen, O. Juliussen and H. F. Svendsen, *Chem. Eng. Sci.*, 2008, **63**, 2641–2656.
- 75 B. Huepen and E. Y. Kenig, *Ind. Eng. Chem. Res.*, 2010, **49**, 772–779.
- 76 J. Gabrielsen, M. L. Michelsen, E. H. Stenby and G. M. Kontogeorgis, *Ind. Eng. Chem. Res.*, 2005, **44**, 3348–3354.
- 77 A. Penttilä, C. Dell’Era, P. Uusi-Kyyny and V. Alopaeus, *Fluid Phase Equilib.*, 2011, **311**, 59–66.
- 78 S. S. Laddha, J. M. Diaz and P. V. Danckwerts, *Chem. Eng. Sci.*, 1981, **36**, 229–230.
- 79 G. F. Versteeg, P. M. M. Blauwhoff and W. P. M. van Swaaij, *Chem. Eng. Sci.*, 1987, **42**, 1103–1119.
- 80 S. J. Park, H. Y. Shin, B.-M. Min, A. Cho and J.-S. Lee, *Korean J. Chem. Eng.*, 2009, **26**, 189–192.
- 81 D. Q. Kern, *Process Heat Transfer*, McGraw-Hill, New York, 1950, p. 871.
- 82 R. K. Sinnott, in *Coulson and Richardson’s Chemical Engineering*, Butterworth-Heinemann, Oxford, 4th edn, 2005, ch. Heat-Trans.
- 83 J. C. Chen, *Ind. Eng. Chem. Process Des. Dev.*, 1966, **5**, 322–329.
- 84 R. Lockhart and R. Martinelli, *Chem. Eng. Prog., Symp. Ser.*, 1949, **45**, 39–48.
- 85 H. K. Forster and N. Zuber, *AIChE J.*, 1955, **1**, 531–535.
- 86 J. R. Couper, in *Chemical Process Equipment Selection and Design*, ed. J. R. Couper, Butterworth-Heinemann, 2nd edn, 1990, ch. 21 Cost, pp. 663–690.
- 87 A. Annut, *Prices of fuels purchased by major power producers*, 2016, <https://www.gov.uk/government/statistical-data-sets/prices-of-fuels-purchased-by-major-power-produce>.
- 88 N. Mac Dowell and N. Shah, *Comput. Chem. Eng.*, 2015, **74**, 169–183.
- 89 C. Kolster, E. Mechleri, S. Krevor and N. Mac Dowell, *Int. J. Greenhouse Gas Control*, 2017, **58**, 127–141.
- 90 E. S. Rubin, J. E. Davison and H. J. Herzog, *Int. J. Greenhouse Gas Control*, 2015, **40**, 378–400.
- 91 E. Crooks, *World’s biggest carbon capture project on schedule*, 2017, <https://www.ft.com/content/eee0d5d6-d700-11e6-944b-e7eb37a6aa8e?mhq5j=e3>.
- 92 P. M. Mathias, K. Afshar, F. Zheng, M. D. Bearden, C. J. Freeman, T. Andrea, P. K. Koech, I. Kutnyakov, A. Zwoster, A. R. Smith, P. G. Jessop, O. G. Nik and D. J. Heldebrant, *Energy Environ. Sci.*, 2013, **6**, 2233–2242.
- 93 P. M. Mathias and J. P. O’Connell, *Ind. Eng. Chem. Res.*, 2012, **51**, 5090–5097.
- 94 A. Zakeri, A. Einbu, P. O. Wiig, L. E. Øi and H. F. Svendsen, *Energy Procedia*, 2011, **4**, 606–613.
- 95 J. Yang, X. Yu, L. An, S.-T. Tu and J. Yan, *Appl. Energy*, 2017, **194**, 9–18.
- 96 S. Freguia and G. T. Rochelle, *AIChE J.*, 2003, **49**, 1676–1686.
- 97 International Energy Agency, *CO2 emissions from fuel combustion highlights. 2015 Edition*, International energy agency technical report, 2015.

